Steam Reforming of Raw Bio-oil in a Fluidized Bed Reactor with Prior Separation of Pyrolytic Lignin

ARTICLE *in* ENERGY & FUELS · DECEMBER 2013

Impact Factor: 2.79 · DOI: 10.1021/ef401835s

energy&fuels

Article

pubs.acs.org/EF

Steam Reforming of Raw Bio-oil in a Fluidized Bed Reactor with Prior Separation of Pyrolytic Lignin

Aingeru Remiro,* Beatriz Valle, A. T. Aguayo, Javier Bilbao, and Ana G. Gayubo

Chemical Engineering Department, University of the Basque Country, P.O. Box 644, 48080, Bilbao, Spain

ABSTRACT: The effect that operating conditions (temperature, steam/carbon molar ratio, and space-velocity) have on the steam reforming of raw bio-oil has been studied in a two-step reaction unit. In the first step (operated at 500 °C), a carbonaceous solid (pyrolytic lignin) deposits by repolymerization of certain bio-oil components, and the remaining volatiles are reformed in the second step (fluidized bed reactor) on a Ni/La_2O_3−αAl_2O_3 catalyst. Under suitable reforming conditions (700 °C, S/C = 9, space-velocity = 8000 h^{-1}), the yields of H_2 and CO were 95% and 6%, respectively. Catalyst deactivation was very low, whereby the H_2 yield decreased by only 2% over 100 min of reaction. By using dolomite as adsorbent in the reforming reactor, CO_2 was effectively captured, and the raw bio-oil was reformed at 600 °C without adding water (S/C = 1.1), thus avoiding its vaporization cost. The yields of H_2 and CO were 80−82% and 1%, respectively, for a space-velocity (G_{C1}HSV) of 7000 h^{-1} and catalyst/dolomite ratio of 0.25, although a high yield of CH_4 (7%) was obtained due to the cracking capacity of the dolomite. The coke content on the catalyst was high (7.7 wt % in 2 h) because of the limited gasification of coke precursors under the operating conditions (low temperature and low S/C ratio) used in the process with CO_2 capture.

1. INTRODUCTION

The H_2 production from fossil sources by reforming of natural gas and petroleum products is increasing, resulting in higher CO_2 emissions.[1,2] Nowadays, greater H_2 production is necessary to satisfy its growing demand, as a fuel and petrochemical raw material. Consequently, new routes from renewable sources (with low CO_2 emissions) are required. For this purpose, the lignocellulosic biomass provides different valorization alternatives.[3−9] Among these, the steam reforming of the bio-oil obtained by flash pyrolysis of biomass has good prospects for industrial implementation, because this bio-oil is obtained by simple technologies (easy to install and transport in case of delocalized use), which have reached a high development level.[10−13] Moreover, the steam reforming avoids the costly separation of water, which is required in other routes for valorizing bio-oil to produce fuel or feedstock in cracking and hydrocracking refinery units.[14−17]

The stoichiometry of raw bio-oil reforming reaction is:

$$C_nH_mO_k + (n - k)H_2O \rightarrow nCO + \left(n + \frac{m}{2} - k\right)H_2 \quad (1)$$

This reaction is followed by the water−gas shift reaction (WGS):

$$CO + H_2O \Leftrightarrow CO_2 + H_2 \quad (2)$$

Thus, the overall steam reforming can be represented as follows:

$$C_nH_mO_k + (2n - k)H_2O \rightarrow nCO_2 + \left(2n + \frac{m}{2} - k\right)H_2 \quad (3)$$

Additionally, there are secondary reactions:

$$\text{cracking: } C_nH_mO_k \rightarrow C_xH_yO_z + \text{gas } (H_2, CO, CO_2, CH_4, H_xC) + \text{coke} \quad (4)$$

$$\text{methane reforming: } CH_4 + H_2O \Leftrightarrow CO + 3H_2 \quad (5)$$

The Boudouard reaction and cracking reactions of CH_4 and other hydrocarbons should also be considered because of their role in coke formation.

$$2CO \Leftrightarrow CO_2 + C \quad (6)$$

$$CH_4 \Leftrightarrow C + H_2 \quad (7)$$

$$H_xC \Leftrightarrow \text{coke precursors (olefins + aromatics)} \rightarrow C + \frac{x}{2}H_2 \quad (8)$$

Knowledge of the fundamentals of bio-oil reforming (such as the behavior of different catalysts based on Ni and noble metals) has been gained in the last two decades, thanks to the reforming studies of model oxygenates (acetic acid, phenol, acetol, etc.)[18−25] and bio-oil aqueous fraction,[26−32] composed of light oxygenates that are soluble in water.[33] However, there are scarce studies on the reforming of raw bio-oil (without prior treatment) because of the repolymerization of certain bio-oil compounds (derived from biomass lignin) that leads to the formation of carbonaceous solid (pyrolytic lignin). This deposition increases the catalyst deactivation, and it can even block the reactor. The previous thermal treatment of the raw bio-oil makes pyrolytic lignin to be deposited isolately. However, this treatment causes a loss of hydrogen content liable to valorization by reforming.[34]

Received: September 13, 2013
Revised: November 11, 2013
Published: November 11, 2013

   dx.doi.org/10.1021/ef401835s | *Energy Fuels* 2013, 27, 7549−7559

To prevent the pyrolytic lignin deposition, caused by raw bio-oil vaporization, different strategies have been used at laboratory scale: (i) the cofeeding of methanol and bio-oil;[35] (ii) the operation in reforming−regeneration cycles (by solid deposits combustion);[15,36] and (iii) the operation with two reactors in line, with a controlled deposition in the first step, so that the catalyst suffers lower deactivation in the subsequent step.[37−41] In this Article, the latter strategy has been applied by using a first step for pyrolytic lignin repolymerization and a subsequent fluidized bed catalytic reactor for reforming the volatile stream coming from the thermal step. The efficiency of this two-step system for reforming the bio-oil aqueous fraction on a $Ni/La_2O_3-\alpha Al_2O_3$ catalyst was previously proven,[42] and the suitable operating conditions for attaining full bio-oil conversion with maximum H_2 yield were also determined.[43] Moreover, the use of a fluidized bed reactor allows incorporating an adsorbent (dolomite), and thereby the reforming with in situ CO_2 capture through CaO carbonation reaction:

$$CaO + CO_2 \Leftrightarrow CaCO_3 \quad (9)$$

The CO_2 capture is able to shift the thermodynamic equilibrium of the reactions involved in bio-oil reforming (eqs 1 and 2), thus increasing the H_2 yield. The interest of using dolomite for this purpose was already described for the bio-oil aqueous fraction reforming in fixed bed reactor.[44] In a previous paper of the steam reforming of bio-oil aqueous fraction by using dolomite as CO_2 adsorbent,[45] the relationship between reforming/WGS reactions, activated by the catalyst (eqs 1 and 2), and reforming/cracking reactions (eq 4) on the adsorbent was analyzed. It was concluded that a minimum catalyst/dolomite mass ratio of 0.17 is required for attaining a high H_2 yield with low catalyst deactivation.

The objective of this Article is to study the effect of operating conditions (temperature, S/C, and space-velocity) on the reforming of the raw bio-oil in a continuous regime by using an original two-step (thermal-catalytic) reaction system, with a previous separation of pyrolytic lignin in the first step. Specifically, the effect operating variables have on the reaction indices (such as bio-oil conversion and product yields) is analyzed. Furthermore, the effect of dolomite incorporation into the fluidized reforming reactor (aimed at increasing the H_2 yield by CO_2 capture) has been studied. Special emphasis has been placed on the catalyst deactivation by coke deposition and also on analyzing the effect operating conditions and reaction medium composition have on this deactivation.

2. EXPERIMENTAL SECTION

2.1. Bio-oil Production and Composition. Bio-oil was obtained by flash pyrolysis of pine sawdust at 480 °C in a semi-industrial demonstration plant, located in Ikerlan-IK4 technology center (Alava, Spain), with a biomass feeding capacity of 25 kg h^{-1}.[46] This plant was developed on the basis of previous results obtained in a laboratory plant (120 g h^{-1}).[47,48] The raw bio-oil composition was determined by a GC/MS analyzer (Shimadzu QP2010S device), and it is shown in Table 1, on a water-free basis. The composition of the bio-oil exiting the thermal treatment step at 500 °C ("treated bio-oil") is also shown. In this thermal step, 23 wt % of the raw bio-oil oxygenates was deposited (as pyrolytic lignin). The corresponding molecular formulas are $C_{4.3}H_{7.2}O_{2.6}$ and $C_{3.5}H_{8.4}O_{3.1}$ (water-free basis) for the raw bio-oil and the treated bio-oil, respectively. The water content in raw bio-oil, determined by Karl Fischer valorization (KF Titrino Plus 870), was 35 wt %.

Table 1. Composition (wt %) of the Raw Bio-oil and Treated Bio-oil after Thermal Treatment at 500 °C

compound/group	raw bio-oil	treated bio-oil
acetic acid	12.8	15.7
acetone	5.5	7.2
1-hydroxy-2-propanone	16.3	13.6
hydroxyacetaldehyde	8.5	5.6
methanol	1.3	0.3
levoglucosan	11	19.7
other ketones	3.8	3.5
other acids	4.0	4.8
other alcohols	2.4	1.3
other aldehydes	6.5	5.8
esters	5.1	1.9
ethers	1.4	2.3
phenols	16.6	14.7
others	2.3	1.9
nonidentified	2.6	1.7

2.2. Catalyst and Dolomite. The $Ni/La_2O_3-\alpha Al_2O_3$ catalyst was prepared with 10 wt % of Ni and 9 wt % of La_2O_3 by using the method described previously by Valle et al.,[42] which was established by Alberton et al.[49] The $La_2O_3-\alpha Al_2O_3$ support was obtained by impregnation of α-Al_2O_3, under vacuum at 70 °C, with an aqueous solution of $La(NO_3)_3{\cdot}6H_2O$ (Alfa Aesar, 99%), followed by drying at 100 °C for 24 h and calcination at 900 °C for 3 h. Subsequently, an impregnation with $Ni(NO_3)_2{\cdot}6H_2O$ and drying at 110 °C for 24 h were carried out, and the final catalyst was calcined at 700 °C for 3 h. The catalyst was reduced at 700 °C for 2 h, by using a H_2−He flow (5 vol % of H_2), prior to each reforming reaction. Subsequently, a He flow was established to remove the H_2 that might have been retained.

The catalyst properties were previously described in detail by Valle et al.[42] The physical properties, such as BET surface area (34.8 m^2 g^{-1}) and pore volume (0.171 cm^3 g^{-1}), were evaluated from the N_2 adsorption−desorption isotherms by using a Micromeritics ASAP 2010C analyzer. This device was also used for hydrogen chemisorption measurements for quantifying Ni dispersion and metallic surface, with the resulting values of 5.1% and 3.7 m^2 g^{-1}, respectively.

The TPO (temperature programmed oxidation) analyses of the coke deposited on the deactivated catalyst were conducted by combustion with air in a Setaram TG-DSC-11 Calorimeter coupled to a mass spectrometer Thermostar Balzers Instrument for monitoring the signals corresponding to mass 18 (H_2O) and 44 (CO_2). For severely deactivated catalyst samples (coke contents >5 wt %), the coke was analyzed by thermogravimetry (combustion with air) in a TA Instruments Q5000 IR thermobalance.

The dolomite used in this Article was provided by Calcinor S.A. (Tolosa, Spain) with particle size <3 mm and density of 2.8 g cm^{-3}. Dolomite composition (wt %) was: $CaCO_3$, 58; $MgCO_3$, 36; Fe_2O_3, 0.3; S, 0.07. Prior to its use, the dolomite was sieved (90−150 μm) and calcined at 800 °C for 2 h to obtain the active phase (CaO).

2.3. Reaction System. The reaction equipment consists of two reactors in-line (Figure 1), and it has been previously described in detail.[43] The first reactor (thermal treatment of bio-oil) retains the carbonaceous solid (pyrolytic lignin) formed by repolymerization of certain bio-oil oxygenates. The volatile compounds that leave this thermal step are subsequently transformed (by catalytic steam reforming) in the second unit (fluidized bed reactor). The controlled deposition of pyrolytic lignin in a specific thermal step, prior to the catalytic reactor, minimizes the operating problems caused by this deposition and attenuates catalyst deactivation. This fact was previously verified for the catalytic conversion of raw bio-oil into hydrocarbons.[41,50,51]

The online analysis of the reforming products was carried out continuously (more representative and stable than discontinuous sampling) with a gas chromatograph (Agilent Micro GC 3000) provided with four modules for the analysis of the following: (1)

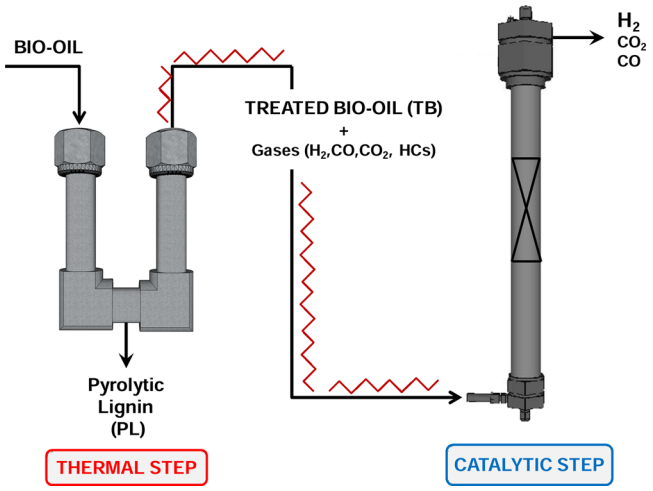

Figure 1. Scheme of the two-reactor system.

permanent gases (O_2, H_2, CO, and CH_4) with 5A molecular sieve capillary column; (2) light oxygenates (C_{2-}), CO_2, and water, with Plot Q capillary column; (3) C_2−C_4 hydrocarbons, with alumina capillary column; and (4) oxygenated compounds (C_{2+}) with Stabilwax type column. The mass balances, calculated from the chromatographic analysis of the bio-oil fed and of the product stream that leaves the reforming reactor, were closed at ≥95 wt % in all experiments.

The experimental two-unit system was operated at atmospheric pressure, and the bio-oil feeding rate (0.1 mL min^{-1}) was controlled by an injection pump Harvard Apparatus 22. The particle size of catalyst and dolomite (obtained by sieving) was 150−250 and 90−120 μm, respectively. An inert solid (CSi, with 30−50 μm particle size) was also used in the reactor, in inert/catalyst or inert/(catalyst + dolomite) mass ratio of 4/1 or 1/1, respectively, to improve the hydrodynamic properties of the catalytic bed. The particle sizes of the three solids are suitable for bed hydrodynamics and for allowing their separation after reaction, required for their individual characterization.

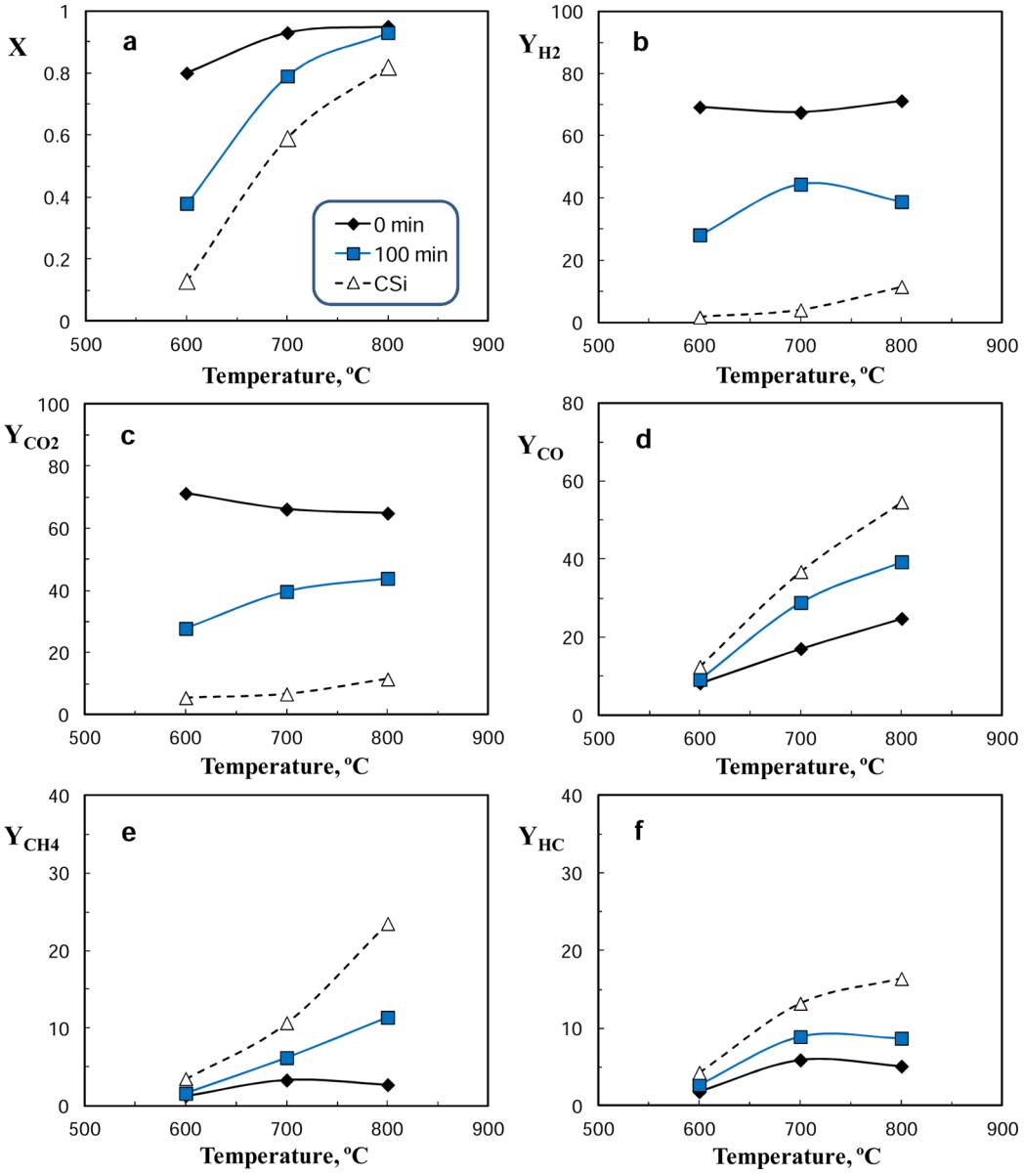

Figure 2. Effect of temperature on bio-oil conversion (a) and yields of H_2 (b), CO_2 (c), CO (d), CH_4 (e), and hydrocarbons (f), at 0 and 100 min time on stream by using CSi (without catalyst). Reaction conditions: S/C, 9; G_{C1}HSV, 155 000 h^{-1}.

dx.doi.org/10.1021/ef401835s | *Energy Fuels* 2013, 27, 7549−7559

3. RESULTS

3.1. Reaction Indices. To quantify the results, the following reaction indices were used:

$$\text{bio-oil conversion: } X = \frac{F_{\text{inlet}} - F_{\text{outlet}}}{F_{\text{inlet}}} \quad (10)$$

where F is the molar flow-rate of bio-oil oxygenates, in C units.

$$\text{hydrogen yield: } Y_{H_2} = \frac{F_{H_2}}{F^{o}_{H_2}} \times 100 \quad (11)$$

where F_{H_2} is the molar flow-rate of H_2 in the product stream and $F_{H_2}{}^{o}$ is the stoichiometric maximum of the bio-oil fed to the reactor (full conversion in eq 3).

The yield of each C-containing product (CO_2, CO, CH_4, and hydrocarbons, mainly ethane and ethylene):

$$Y_i = \frac{F_i}{F_{\text{inlet}}} \times 100 \quad (12)$$

where F_i is the molar flow-rate of each compound, and F_{inlet} is the molar flow-rate of the bio-oil fed into the reactor, in C units.

$$\text{hydrogen productivity: } P_{H_2} = \frac{F_{H_2}}{m_{\text{bio-oil}}} \quad (13)$$

where $m_{\text{bio-oil}}$ is the mass flow-rate of the bio-oil fed (water-free basis).

The experimental errors determined by repeated experiments are ±3% in the H_2 yield values and ±1% in those of C-containing products.

3.2. Effect of Reaction Conditions. The temperature of the thermal treatment step was 500 °C, and the catalytic steam reforming conditions were: temperature, 600, 700, 800 °C; bio-oil flow-rate, 0.1 mL min^{-1}; steam/carbon molar ratio, 1−15 (varying the water flow-rate in the 0−0.3 cm^3 min^{-1} range); space-velocity ($G_{C1}HSV$), 8000−156 000 h^{-1} (in CH_4 equivalent units), which corresponds to a catalyst mass in the 0.1−1.0 g range. High values of space-velocity were used to clearly observe the effect of other operating variables on the catalyst deactivation by coke.

3.2.1. Temperature. Figure 2 shows the effect of temperature on bio-oil conversion (Figure 2a) and on the yields of H_2 (b), CO_2 (c), CO (d), CH_4 (e), and hydrocarbons (mainly ethane and ethylene) (f) at zero time on stream (fresh catalyst) and after 100 min reaction. It should be noted that the first chromatographic analysis is obtained at around 5 min time on stream, and this result is considered as that corresponding to "zero" time on stream. The results without catalyst (i.e., by using only inert CSi in the reactor) are also shown (dashed lines) to highlight the significance of bio-oil thermal decomposition reactions, which are noticeably enhanced with temperature.

These results reveal that bio-oil conversion without catalyst is significant above 600 °C, with CO, CH_4, and hydrocarbons being the major products. The use of a catalyst increases conversion and is a key factor to modify product distribution, with the formation of H_2 and CO_2 as major products due to the reforming of CH_4 and hydrocarbons.

High bio-oil conversion (>0.8) is obtained with the fresh catalyst in the whole temperature range, with values being higher as the temperature is increased (Figure 2a). The decrease in bio-oil conversion after 100 min reaction is very pronounced at 600 °C, lower at 700 °C, and negligible at 800 °C because the catalyst deactivation is attenuated with increasing temperature, as explained later in detail.

The H_2 yield at zero time on stream is similar for all temperatures studied (∼70%) and is around 10% at 800 °C without catalyst, which reveals a low H_2 selectivity from the bio-oil thermal decomposition (Figure 2b). These experiments correspond to a high value of space-velocity (155 000 h^{-1}); thus there is a rapid catalyst deactivation for reforming and WGS reactions, which causes the remarkable decrease in H_2 yield throughout 100 min. The lowest deactivation is observed at 700 °C.

The CO_2 yield obtained with fresh catalyst (t = 0) decreases slightly with temperature (Figure 2c) because the WGS reaction is disfavored, thus increasing the yield of CO (Figure 2d). The yields of CH_4 (Figure 2e) and hydrocarbons (Figure 2f) obtained with fresh catalyst show a less pronounced trend with temperature, with a maximum at 700 °C. The yields of CH_4 (Figure 2e) and hydrocarbons (Figure 2f) obtained without catalyst are noticeable, with values that increase with temperature (especially above 600 °C). These byproducts are more effectively reformed at higher temperatures. Ethylene is the major compound in the hydrocarbons lump, followed by propylene and ethane, and low amounts of propane and butane. Furthermore, the effect of temperature causes a marked increase in ethylene content from 60% at 600 °C to 90% at 800 °C.

After 100 min of reaction, the yields of H_2 and CO_2 decrease and the yields of CO, CH_4, and HCs increase, because the catalyst is partially deactivated for reforming and WGS reactions. Under these conditions, thermal cracking reactions of the bio-oil oxygenates present in the reaction medium (eq 4) become more significant. This cracking is greater at higher temperatures, increasing significantly the yields of CO (Figure 2d), CH_4 (Figure 2e), and HCs to a lesser extent (Figure 2f). These results reveal the dependence between the catalytic reactions (reforming and WGS) and thermal decomposition reactions, whose products are catalytically transformed.

These deactivation results suggest that the optimum temperature is around 700 °C to strike a balance between the severe decrease in bio-oil conversion at low temperature (600 °C) and the high byproduct yields (CO, CH_4, and HCs) at high temperature (800 °C). Coke formation (eq 8) plays an important role in the catalyst deactivation and is enhanced by increasing temperature until gasification of coke precursors and coke (reverse eqs 6 and 7) becomes significant, which is also favored by higher temperatures.

Figure 3 shows the TPO results of the coke deposited at 600 and 700 °C, with coke contents of 3.35 and 1.14 wt %, respectively. The TPO of the coke deposited at 800 °C is not shown due to its negligible coke content (∼0.1 wt %). These results confirm that coke deposition (and thus deactivation) is lower at higher reaction temperatures because gasification prevails over coke formation.

The TPO profile of the coke deposited at 600 °C shows three peaks at 292, 391, and 570 °C, respectively. The position of combustion peaks in supported metal catalysts and bifunctional catalysts is related to the proximity between the metal and the coke and to the metal ability to activate coke combustion. Consequently, the peak at 292 °C is associated with a coke fraction deposited on the Ni sites, and its combustion is catalyzed by this metal. The peak at 391 °C is

dx.doi.org/10.1021/ef401835s | Energy Fuels 2013, 27, 7549−7559

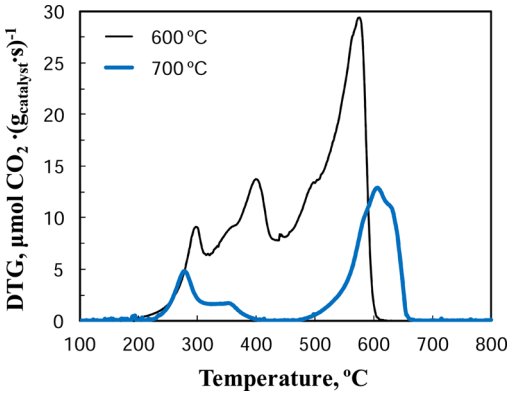

Figure 3. Temperature programmed oxidation (TPO) profiles of the coke deposited on the catalyst at 600 and 700 °C. Reaction conditions: S/C, 9; $G_{C1}HSV$, 155 000 h^{-1}; time on stream, 100 min.

related to the coke deposited outside of the catalyst particle (named pyrolytic lignin, according to its origin, or external coke, according to its location). This coke burns at lower temperature than the coke fraction deposited on the La_2O_3–αAl_2O_3 support (peak at 570 °C), whose combustion is not activated by Ni metal sites. The coke deposited at 700 °C has a different structure because the intermediate peak (391 °C) is not observed and the peaks at low and high temperatures are shifted to 271 and 605 °C, respectively. This is a consequence of coke gasification, which causes less coke deposition on the catalyst at 700 °C, and is almost negligible at 800 °C.

The identification of three peaks in coke combustion, corresponding to fractions in different locations (on the outside of the particle, inside the particle covering the metal, and inside the particle covering the support), is characteristic of metallic and bifunctional catalysts, such as CuO–ZnO–Al_2O_3/γ-Al_2O_3 used in the synthesis of DME.[52,53] Only two fractions are identified over acid catalysts, external and internal (also known as thermal and catalytic, according to their origin), as Valle et al.[54] reported for the raw bio-oil transformation over HZSM-5 zeolite.

On the basis of the above results, a scheme of the reaction steps involved in the catalyst deactivation by coke deposition is proposed in Figure 4. The coke consists of aromatic condensates, which are presumably formed by two causes: (i) pyrolytic lignin deposition (mainly outside of the catalyst particles), which is not entirely avoided with the previous thermal treatment step at 500 °C; this deposition may also partially occur inside the catalyst particle, by repolymerization of the phenolic derivatives (coming from lignin pyrolysis) of lower molecular weight; and (ii) condensation (activated by the dehydrogenating capacity of the catalyst) of hydrocarbons formed by cracking of bio-oil oxygenates (eq 8). The olefins and aromatics capacity for forming coke is well-known, which is favored with increasing temperature.[55] The Boudouard reaction (eq 6) and the CH_4 cracking (eq 7) also presumably contribute to the coke formation at high temperature.

Coke formation reactions are favored by increasing temperature, but gasification of the coke precursors adsorbed on the catalyst is further enhanced in the range studied. Thereby, coke formation at 700 °C is significantly lower than that at 600 °C (Figure 3). Coke formation is negligible at 800 °C, and, at this temperature, the Ni sintering causes the catalyst deactivation. Accordingly, the catalyst used at 600 and at 700 °C recovers its metallic properties upon coke combustion with air at 600 °C, whereas the catalyst used at 800 °C shows a higher average Ni particle size (12.1 nm) than the fresh catalyst (7.9 nm).

3.2.2. Steam/Carbon Molar Ratio (S/C). The effect of S/C molar ratio was studied by feeding 0.1 cm^3 min^{-1} of raw bio-oil and varying the water flow-rate between 0 and 0.3 cm^3 min^{-1}. Figure 5 shows the effect, at 700 °C, on bio-oil conversion, H_2 yield (Figure 5a), and the yields of CO and CO_2 (Figure 5b). The results remain constant with time on stream as they correspond to a low value of space-velocity ($G_{C1}HSV$ = 32 500 h^{-1}) for which deactivation is negligible (with a coke content <0.2 wt %). The yields of CH_4 and C_2 hydrocarbons are also very low (less than 1%) under these conditions.

The bio-oil is fully converted in the whole range of S/C studied, and the product yields are notably affected by this ratio. The yields of H_2 (Figure 5a) and CO_2 (Figure 5b) increase notably with the S/C ratio up to S/C = 5. Above this value, this increase is less relevant (up to H_2 yield of 95% for S/C = 15). Concurrently, there is a marked decrease in CO yield because the WGS reaction (eq 2) is enhanced due to the higher water content in the reaction medium. Higher S/C molar ratios lead to a greater energy cost for water evaporation, so that a S/C ratio ≈ 6 is enough to achieve high bio-oil conversion and H_2 yield, without exorbitant energy cost.

3.2.3. Space-Velocity. The effect of space-velocity ($G_{C1}HSV$) on bio-oil conversion, H_2 yield (Figure 6a), and the yields of CO, CO_2 (Figure 6b), CH_4, and hydrocarbons (Figure 6c) is shown in Figure 6. The results correspond to zero time on stream (fresh catalyst) and 100 min time on stream. The experiments were carried out with S/C = 9, for which a high H_2 yield is achieved (section 3.2.2), so that the effect of space-velocity is not masked by the effect of S/C.

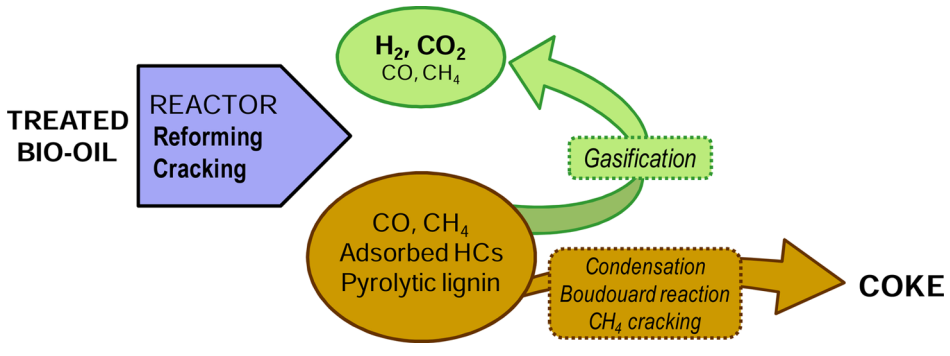

Figure 4. Stages of formation and gasification of coke precursors in the bio-oil reforming.

dx.doi.org/10.1021/ef401835s | *Energy Fuels* 2013, 27, 7549–7559

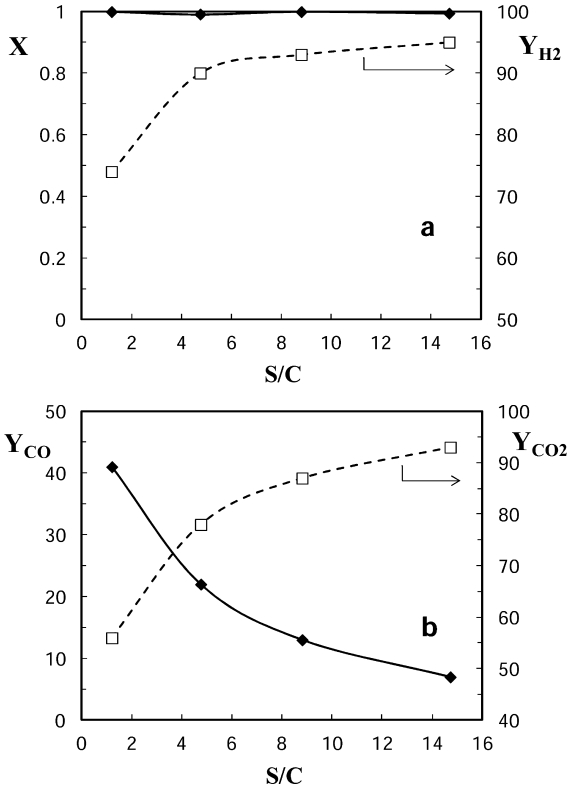

Figure 5. Effect of S/C ratio on bio-oil conversion and H_2 yield (a) and yields of CO_2 and CO (b). Reaction conditions: 700 °C; $G_{C1}HSV$, 32 500 h^{-1}.

The bio-oil conversion at zero time on stream (Figure 6a) is full for space-velocities lower than 65 000 h^{-1}. For the lowest value of space-velocity studied (8000 h^{-1}), the H_2 yield is almost the stoichiometric maximum (~95%, Figure 6a), and the yield of CO is very low (~6%, Figure 6b). This H_2 yield is higher than that obtained by other authors at the same temperature (700 °C) in a single reaction step.[37,56] It should be noted that these results are not directly comparable, because 23 wt % of raw bio-oil oxygenates is removed in the thermal step (at 500 °C) prior to reforming. Furthermore, the thermal treatment used in this Article modifies the raw bio-oil composition, so that the "treated" bio-oil has a lower content of high molecular weight compounds.

The bio-oil conversion (Figure 6a) slightly decreases with increasing space-velocity above 65 000 h^{-1}. The catalyst deactivation does not affect the bio-oil conversion at space-velocities below 32 000 h^{-1}. Above this value, deactivation becomes more pronounced with increasing space-velocity, because the concentration of unreformed oxygenates in the reaction medium is higher, and these compounds are responsible for coke formation.

The initial H_2 yield (t = 0) is lower as the space-velocity is increased (especially for values greater than 32 000 h^{-1}), with resulting values of 95% at $G_{C1}HSV$ = 8000 h^{-1} and 72% at 156 000 h^{-1} (Figure 6a). For low values of space-velocity, the decrease in H_2 yield after 100 min reaction is negligible, although for values above 65 000 h^{-1} this yield significantly drops (to 30% at 156 000 h^{-1}) due to deactivation of reforming and WGS reactions. The initial CO_2 yield (t = 0) steadily decreases with increasing the space-velocity (Figure 6b), with this effect being more noticeable with the deactivated catalyst (after 100 min reaction). The decrease in both reaction

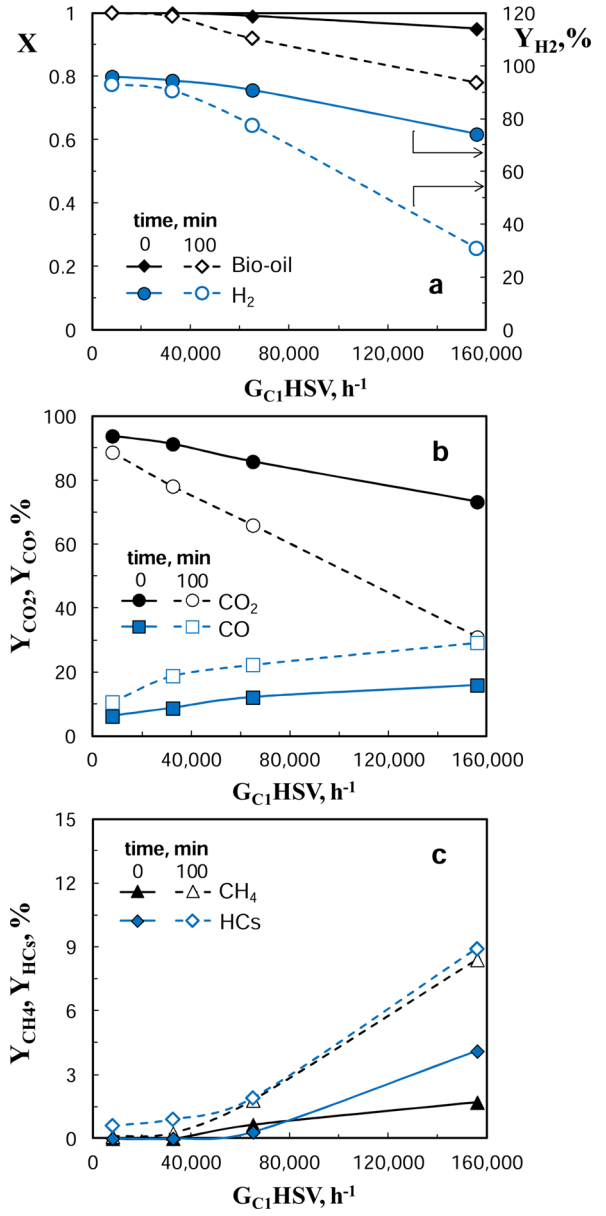

Figure 6. Effect of space-velocity ($G_{C1}HSV$) on bio-oil conversion and H_2 yield (a), CO_2 and CO yields (b), and CH_4 and hydrocarbons yields (c), at 0 and 100 min time on stream. Reaction conditions: 700 °C; S/C, 9.

products (H_2 and CO_2) as time on stream increases is a consequence of the catalyst deactivation for reforming and WGS reactions, which is higher as the space-velocity value is increased. Furthermore, as the catalyst deactivates, the cracking reactions of bio-oil oxygenates (eq 8) become more significant (due to the higher concentration in the reaction medium). Consequently, an increase in space-velocity leads to higher yields of CO, CH_4, and light hydrocarbons (Figure 6b,c). This increase is more noticeable for the partially deactivated catalyst than for the fresh catalyst. No significant effect of the space-velocity is observed on the hydrocarbon product distribution in the lump, with ethylene being the major component (70%).

These deactivation results are consistent with the coke contents deposited on the catalyst (Table 2). Although the increase in space-velocity enhances the coke formation reactions (Figure 4), the coke precursors are efficiently gasified

dx.doi.org/10.1021/ef401835s | Energy Fuels 2013, 27, 7549−7559

Table 2. Effect of Space-Velocity on Coke Content of the Catalyst[a]

$G_{C1}HSV$, h^{-1}	coke, wt %
8000	0.1
32 500	0.2
65 000	0.8
156 000	1.14

[a]Reaction conditions: 700 °C; S/C = 9; time on stream, 100 min.

at 700 °C, and thereby high coke contents (those that may block Ni sites) are only attained for very high values of space-velocity. Therefore, it can be operated in a wide range of space-velocities at 700 °C without a noticeable catalyst deactivation by coke.

3.3. Comparison of Raw Bio-oil and Aqueous Fraction Reforming. Figure 7 compares the mass balances of the two-step process for the steam reforming of: (i) raw bio-oil (this Article), and (ii) the aqueous fraction of bio-oil (obtained after adding water to raw bio-oil in mass ratio 2/1).[43] In both cases, 100 g of raw bio-oil (considering the water content) is taken as a basis for calculation. The greatest differences in these alternatives are: (a) the separation of a water insoluble fraction (organic fraction) when the aqueous fraction is valorized; this fraction retains 23 wt % of bio-oil oxygenates (mainly phenolics and with high molecular weight); (b) the yield of pyrolytic lignin (deposited in the thermal step at 500 °C) is 17 wt % for the aqueous fraction[43] and 23 wt % for the raw bio-oil. As a result, although similar H_2 yields are obtained in the catalytic reforming step (96% for aqueous fraction[43] and 95% for raw bio-oil), the H_2 productivity (eq 13) referred to the raw bio-oil (in a water-free basis) is different: 50.5 $mmol_{H2}/g_{bio\text{-}oil}$ (6.57 gH_2/100 g of raw bio-oil considering water) for the aqueous fraction reforming and 58.6 $mmol_{H2}/g_{bio\text{-}oil}$ (7.62 gH_2/100 g of raw bio-oil considering water) for the reforming of the raw bio-oil. However, it should be considered that the aqueous fraction reforming involves fewer operational problems (caused by the carbonaceous solid deposition) and the catalyst deactivation is low. This allows a longer operation time before catalyst regeneration is required (to maintain a high H_2 yield).

Furthermore, to compare both strategies at their optimum conditions, it is necessary to study the alternatives for valorizing both the organic fraction of bio-oil (separated by the aqueous treatment) and the pyrolytic lignin (deposited in the thermal step). Both fractions are interesting for energetic valorization, extraction of components (such as phenolic compounds for obtaining phenolic resins), and gasification aimed at obtaining methanol (used as a stabilizer in storing bio-oil).

3.4. Comparison of Technologies for Reforming Raw Bio-oil. Table 3 summarizes the results in the literature of the H_2 concentration in the product stream (C_{H2}), H_2 productivity (referred to the raw bio-oil fed, P_{H2}), and H_2 yield (referred to the stoichiometric value of the raw bio-oil in the feed, Y_{H2}). The main features of the corresponding process (type of reactor, catalyst composition, temperature, S/C ratio, and space-velocity) are also shown.

Because the differences in operating strategy (one or two steps, with prior gasification in some cases), the type of reforming reactor (fixed or fluidized), and the reaction conditions, it is difficult to compare the mass balances and

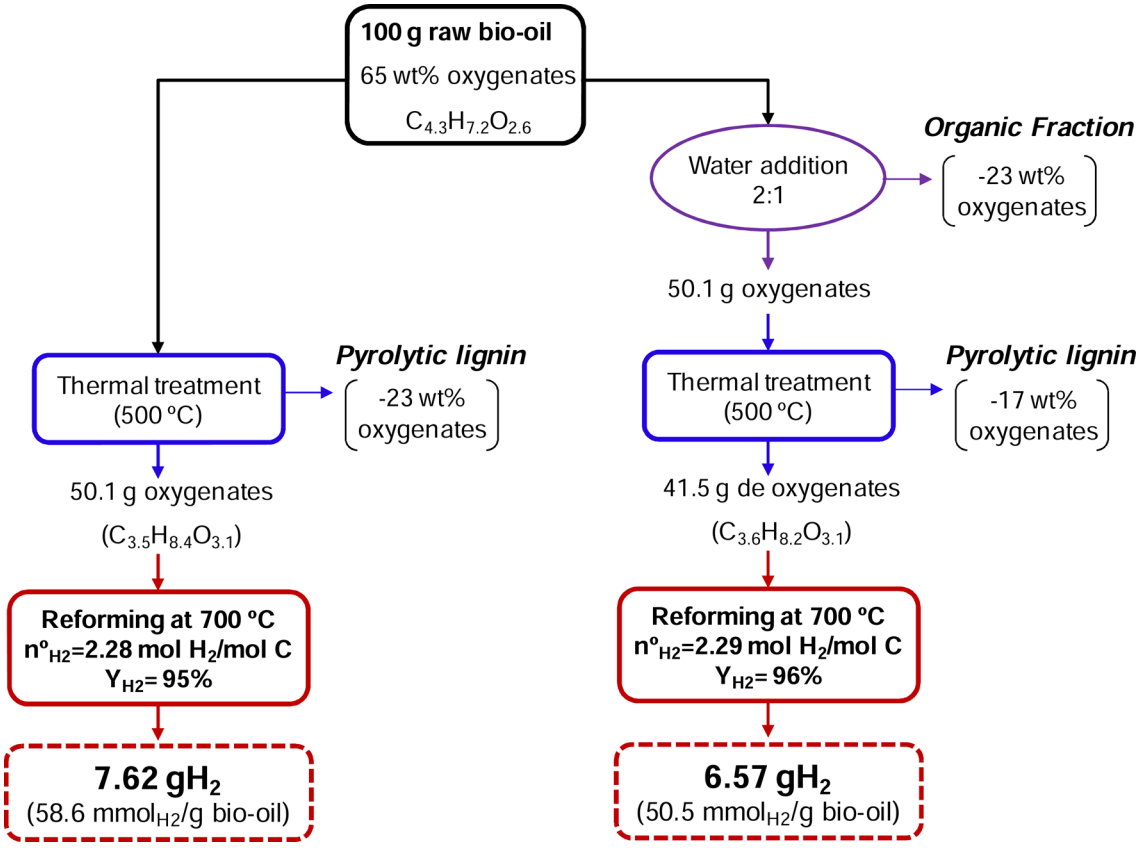

Figure 7. Comparison of H_2 yields obtained in the reforming of the bio-oil aqueous fraction and the raw bio-oil by using the two-step process (thermal + reforming).

dx.doi.org/10.1021/ef401835s | Energy Fuels 2013, 27, 7549−7559

Table 3. Comparison of Results Reported in the Literature on the Steam Reforming of Raw Bio-oil

ref	reactor	metal	support	T, °C	S/C	GHSV, h^{-1}	C_{H2}, vol %	P_{H2}, mmol $g_{bio\text{-}oil}^{-1}$	X, %	Y_{H2}, %
18	fixed bed	Pt (1%)	$CeZrO_2$	860	5.0	3090		58[a]		60
					10.8	3090		69[a]		72
			Al_2O_3	860	10.8	3090		25[a]		28
		Rh (1%)	$CeZrO_2$	860	10.8	3090		73[a]		76
			Al_2O_3	860	10.8	3090		59[a]		62
57	fixed bed	Ni−K (4%−2%)	$La_2O_3Al_2O_3$	700	0.7	10[b]	49.2	18	100	40
36	monolithic (cordierite)	Pt (1%)	$Ce_{0.5}Zr_{0.5}O_2$	700	0.7	10[b]	49	17	100	45
		Rh (1%)				10[b]	52	18	100	48
58	fixed bed[c]	Ni[d]		809	3.2	0.1[b]	55.5	41.5	76	46
37	fixed bed	Mg (18%)	CaO Al_2O_3	750	4	10000		54.2	96	80
35	fluidized bed	Ni−K−Mg	C11−NK[e]	850	5.8	920	70	64.5	95	80
15	monolithic (cordierita)	Pt (1%)	$Ce_{0.5}Zr_{0.5}O_2$	780	10	5[b]	67	67.5	100	70
		Rh (1%)	$Ce_{0.5}Zr_{0.5}O_2$	780	10	5[b]	65	50.1	100	52
38	fixed bed[f]	Ni (7.2%)	MgO	850	16	3600		45.5	100	81
59	fixed bed[g]	Ni (15%)	CNTs	550	6.1	12 000	68.1	53[a]	94.9	92.5[h]
40	fixed bed[c]	Ni−Cu−Zn (33−18−19%)	Al_2O_3	700	10.6	7810	72.5	51.4	74.3	65
60	fixed bed	Ni (14%)	Al_2O_3	950	5	13[b]		61.4[a]	79	73
61	fixed bed	Ni−Ru (14%−0.5%)	Al_2O_3	950	5	13[b]		71.9[a]	81	85
		Ni−Mg (33%−13%)		950	5	13[b]		63.4[a]	79	75
62	fixed bed	Ni (3%) Co (9%)	CeO_2−ZrO_2	850	2	2.62[c]	57.6			72
63	fixed bed	Ni (14%)	ZrO_2	850	5	13[b]	65.2	49.5[a]		79[i]
this work	fluidized bed	Ni (10%)	La_2O_3−αAl_2O_3	700	9	8000/7[b]	71	58.6	100	95[h]/61

[a]Calculated from Y_{H2} and bio-oil composition. [b]WHSV, h^{-1}. [c]After gasification step at 800 °C. [d]Catalyst K46, naphtha reforming commercial catalyst. [e]Naphtha reforming commercial catalyst. [f]After preliminary reforming with dolomite (900 °C, S/C = 16, WHSV = 1.5 h^{-1}). [g]Reforming of volatile fraction (60 wt % of bio-oil) after vaporization at 180 °C. [h]In the reforming reactor. [i]Potential H_2 yield.

the feasibility of various alternatives. Furthermore, to make a rigorous comparison, the catalyst deactivation and analysis of the energy requirements of these alternatives should be considered.

Salehi et al.[61] studied improvements of the Ni/Al_2O_3 catalyst for reforming the raw bio-oil in a fixed bed and found that the addition of Ru to Ni increases C conversion and H_2 yield at lower temperatures. Furthermore, these authors analyzed in detail the problem of catalyst deactivation by coke deposition when the raw bio-oil is directly fed into the fixed-bed reactor. The role of the support is noteworthy, given that coke deposition is lower when Al_2O_3 is used than when ZrO_2 is used.[63] In addition, coke content decreases by increasing the S/C ratio above 1, given that coke gasification is enhanced.[60]

The fluidized bed reactor has good performance for mitigating the catalyst deactivation by promoting coke gasification. The two-step process also has good prospects, as was suggested by Van Rossum et al.[39] and Kan et al.[40] who used a first gasification step (at around 800 °C) and a second step to reform the exiting volatile stream.

The process proposed in this Article, with a previous step of pyrolytic lignin separation, is a simple alternative aimed at minimizing the problem of catalyst deactivation by coke (key factor for the viability of the raw bio-oil reforming process). A H_2 yield of 95% is obtained in the reforming step, and this H_2 yield, referred to as the raw bio-oil fed, is 61% at a moderate temperature of 700 °C required for minimizing Ni sintering. Furthermore, the pyrolytic lignin separated in the first step can be valorized by treatments similar to those used for lignins obtained as byproduct in the paper industry,[41] which contributes to the economic viability of the process. The operational problems in the reforming reactor are similar to those in the reforming of the bio-oil aqueous fraction,[26−32] although a rigorous comparison of both strategies would require a custom economic study.

3.5. Steam Reforming with CO_2 Capture. In the bio-oil reforming with CO_2 capture, the catalytic reactions (reforming and WGS) and thermal reactions (bio-oil oxygenates cracking) on both solids (catalyst and CO_2 adsorbent) and the CO_2 capture (eq 9) take place in the same reactor. Each of these reactions is affected by deactivation of both catalyst and adsorbent, and coke formation (key factor in the catalyst deactivation) is greatly affected by gasification. Consequently, interpretation of the results obtained in this integrated process is complex, although we have the previous experience on the reforming of the bio-oil aqueous fraction with CO_2 capture in the same two-step reaction system used in this Article.[45] A good behavior of dolomite at 600 °C was proven, and appropriate intervals for operating conditions were established.

In this Article, the thermal step was performed at 500 °C, and the catalytic steam reforming conditions were: 600 °C, S/C = 1.1, space-velocity ($G_{C1}HSV$) = 7.000 h^{-1}, catalyst/dolomite mass ratio = 0.25, and dolomite mass = 6 g. The reforming temperature of 600 °C is suitable for achieving a good carbonation-reforming compromise,[45] although a remarkable catalyst deactivation by coke deposition is expected, according to the results of section 3.2.1. No water was added in the feed, which corresponds to S/C = 1.1 in the reforming reactor feed (41 wt % water and 59 wt % treated bio-oil with $C_{3.5}H_{8.4}O_{3.1}$ molecular formula), to evaluate the ability of the CO_2 capture to enhance the reforming, which is interesting to avoid the cost of the cofed water evaporation.

Figure 8 shows the evolution with time on stream of bio-oil conversion and the yields of products (except that of light hydrocarbons as it is less than 1%).

dx.doi.org/10.1021/ef401835s | Energy Fuels 2013, 27, 7549−7559

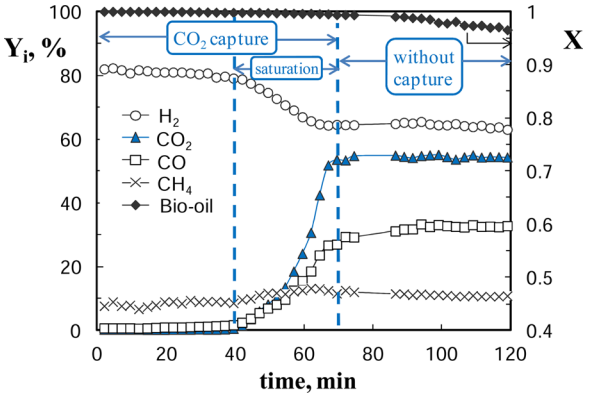

Figure 8. Evolution with time on stream of raw bio-oil conversion and yields of H_2, CO_2, CO, and CH_4. Reaction conditions: 600 °C; S/C, 1.1; $G_{C1}HSV$, 7000 h^{-1}; catalyst/dolomite mass ratio, 0.25; mass of dolomite, 6 g.

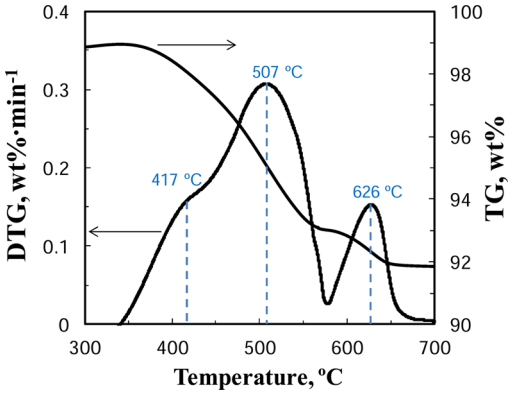

Figure 9. Temperature programmed oxidation (TPO) profile of the coke deposited on the catalyst in the reforming of raw bio-oil with CO_2 capture. Reaction conditions: 600 °C; S/C, 1.1; $G_{C1}HSV$, 7000 h^{-1}; catalyst/dolomite mass ratio, 0.25; mass of dolomite, 6 g.

Considering the evolution with time on stream of CO_2 yield, three successive steps are distinguished: (i) total capture, (ii) breakthrough curve (gradual saturation of dolomite with CO_2), and (iii) total saturation of dolomite (steam reforming without CO_2 adsorption). Consequently, bio-oil is fully converted throughout 70 min, and then it decreases to 0.96 in 2 h. The H_2 yield is 80−82% during the CO_2 capture (with H_2 selectivity of around 95%), and after the dolomite saturation it decreases to 64%. The relevant effect of CO_2 capture on the shift of WGS reaction equilibrium (eq 2) is obvious because the CO yield is minimized (∼1%), whereas this is around 33% without CO_2 capture. This is a high value of CO yield because a very low S/C ratio (S/C = 1.1) is used in the experiment.

The CO_2 yield is 0.3% during the CO_2 capture, and after this period it increases to 55%. The CH_4 yield remains high throughout the reaction, which avoids achieving a higher H_2 yield. Besides, no clear relationship is observed between the CH_4 formation and the CO_2 capture (the CH_4 yield increases from 7% to 13% in 1 h, and then it decreases to 10% in 2 h). This result reveals that the CO_2 capture does not significantly favor the reforming of CH_4, whose formation is due to the dolomite activity for cracking bio-oil compounds (eq 8).[45]

After this reaction (Figure 8), a high coke content on the deactivated catalyst is obtained (7.7 wt %) because its formation is favored by the reaction conditions (Figure 4). It should be noted that the reaction temperature (600 °C) is suitable for the dolomite carbonation, but it also enhances the formation of byproducts (CO, CH_4, hydrocarbons) that are coke precursors (eqs 6−8). Besides, this low temperature and the low steam concentration in the reaction medium (S/C) are not enough for the coke gasification. Furthermore, the adsorbent activity for oxygenates cracking also contributes to this high coke content, as it leads to formation of CH_4 and hydrocarbons (to a lesser extent), which are coke precursors.

Figure 9 shows the TPO results of the coke deposited on the catalyst, with three major peaks at 417, 507, and 626 °C. The most significant is the intermediate peak, which is attributed to the external coke deposited outside the catalyst particle, and is related to the pyrolytic lignin deposition. There are some differences between this result and the TPO of the catalyst deactivated at the same temperature (600 °C) in the reforming without CO_2 capture (Figure 3), which can be explained by the different water content in the reaction medium. Under the operating conditions of the reaction with CO_2 capture (600 °C and S/C = 1.1), the coke precursors and external coke fraction (not in contact with Ni) (peak at high temperature, 626 °C, in Figure 9) are not gasified, whereas the S/C ratio was higher (S/C = 9) and enough to gasify them in the reaction without CO_2 capture; therefore, this peak is not observed in Figure 3.

The aforementioned results reveal the feasibility of the two-step reaction system to reform the raw bio-oil with in situ CO_2 capture and without additional water supply (S/C = 1.1). The yields of H_2, CO, and CO_2 are around 80−82%, 1%, and 0.3%, respectively, with the consequent benefits for hydrogen production (regarding environmental impact and product stream quality). It should be noted that this study was performed under the optimal conditions established previously for the bio-oil aqueous fraction reforming with CO_2 capture,[45] and, therefore, these results of raw bio-oil reforming will presumably be improved under suitable conditions established in future works. Thus, the raw bio-oil reforming will probably require higher catalyst/adsorbent and S/C ratios to minimize the CH_4 formation (aimed at achieving H_2 yields ≈ 100%) and to reduce the deactivation the catalyst by coke deposition. However, the increase in the S/C ratio entails a higher cost of vaporization energy, which must be considered in an economic study.

Furthermore, to implement the process on a larger scale, the reforming step can be performed in a fluidized bed reactor with circulating catalyst, which would be regenerated in another fluidized bed reactor (interconnected to the reforming one) by coke combustion with air diluted in N_2. For the operation with CO_2 capture, the dolomite may also be regenerated by a decarbonation step. This strategy would require separation of dolomite and catalyst (with different size, as in this Article) for their separate regeneration to avoid the irreversible deactivation by Ni sintering that undergoes the catalyst due to the high temperature required for the decarbonation.

4. CONCLUSIONS

The two-step reaction system (thermal-catalytic), with prior separation of pyrolytic lignin in the first step at 500 °C, has proven to be suitable for reforming a raw bio-oil. Under the operating conditions studied, Ni/La_2O_3−αAl_2O_3 catalyst deactivation by coke deposition is only slightly faster than that observed in the reforming of the bio-oil aqueous fraction.

700 °C is the optimum temperature because significant raw bio-oil reforming is achieved, and the coke precursors that

dx.doi.org/10.1021/ef401835s | Energy Fuels 2013, 27, 7549−7559

deactivate the catalyst are gasified, thus limiting the coke deposition. At this temperature, the sintering of Ni/La_2O_3–αAl_2O_3 catalyst is also minimized.

The yields of H_2 and CO_2 increase considerably as the S/C ratio is increased to S/C ≈ 5, with this increase being less pronounced above this value, and the CO yield diminishes as the WGS reaction is favored. As the S/C ratio is increased, the gasification of the coke precursors is also enhanced, thus attenuating catalyst deactivation.

Decreasing space-velocity (G_{C1}HSV) produces higher H_2 yields, with catalyst deactivation being attenuated. The yields of H_2 and CO are ∼95% and ∼6%, respectively, for the lowest value of space-velocity studied (8000 h^{-1}) and S/C = 9. Under these conditions, catalyst deactivation is very low, so the H_2 yield decreases by only 2% over 100 min of reaction.

The process proposed in this Article allows incorporating dolomite in the fluidized bed reforming reactor, thereby increasing the H_2 yield and decreasing the CO yield due to in situ CO_2 capture. This enhancement allows reforming the raw bio-oil at 600 °C without adding water (S/C = 1.1), thus avoiding its vaporization cost. The yields of H_2 and CO were 80–82% and 1%, respectively, for a space-velocity (G_{C1}HSV) of 7000 h^{-1} and a catalyst/dolomite ratio of 0.25, although a high yield of CH_4 (7%) was obtained due to the dolomite cracking capacity. The coke content on the catalyst was high (7.7 wt % in 2 h) because of the low gasification of coke precursors under these operating conditions. This is an encouraging result, although it prompts the need for further studies using higher S/C and catalyst/adsorbent ratios to attain a higher H_2 yield and reduce catalyst deactivation by coke.

AUTHOR INFORMATION

Corresponding Author

*Phone: +34 946 015361. Fax: +34 946 013 500. E-mail: aingeru.remiro@ehu.es.

Notes

The authors declare no competing financial interest.

ACKNOWLEDGMENTS

This work was carried out with the financial support of the Department of Education Universities and Investigation of the Basque Government (IT748-13), of the University of the Basque Country (UFI 11/39), and of the Ministry of Science and Innovation of the Spanish Government (Project CTQ2012-13428/PPQ).

REFERENCES

(1) Levin, D. B.; Chahine, R. *Int. J. Hydrogen Energy* **2010**, *35*, 4962–4969.

(2) Nowotny, J.; Veziroglu, T. N. *Int. J. Hydrogen Energy* **2011**, *36*, 13218–13224.

(3) Ni, M.; Leung, D. Y. C.; Leung, M. k. H.; Sumathy, K. *Fuel Process. Technol.* **2006**, *87*, 461–472.

(4) Navarro, R. M.; Peña, M. A.; Fierro, J. L. G. *Chem. Rev.* **2007**, *107*, 3952–3991.

(5) Dahmen, N.; Dinjus, E.; Kruse, A. Fuels-hydrogen production. Biomass: Thermochemical processes. *Encyclopedia of Electrochemical Power Sources*; Elsevier: New York, 2009; pp 259–267.

(6) Holladay, J. D.; Hu, J.; King, D. L.; Wang, Y. *Catal. Today* **2009**, *139*, 244–260.

(7) Kalinci, Y.; Hepbasli, A.; Dincer, I. *Int. J. Hydrogen Energy* **2009**, *34*, 8799–8817.

(8) Balat, H.; Kirtay, E. *Int. J. Hydrogen Energy* **2010**, *35*, 7416–7426.

(9) Kirtay, E. *Energy Convers. Manage.* **2011**, *52*, 1778–1789.

(10) Anex, R. P.; Aden, A.; Kazi, F. K.; Fortman, J.; Swanson, R. M.; Wright, M. M.; et al. *Fuel* **2010**, *89*, S29–S35.

(11) Butler, E.; Devlin, G.; Meier, D.; McDonnell, K. *Renewable Sustainable Energy Rev.* **2011**, *15*, 4171–86.

(12) Bridgwater, A. V. *Biomass Bioenergy* **2012**, *38*, 68–94.

(13) Meier, D.; van de Beld, B.; Bridgwater, A. V.; Elliott, D. C.; Oasmaa, A.; Preto, F. *Renewable Sustainable Energy Rev.* **2013**, *20*, 619–641.

(14) Corma, A.; Huber, G. W.; Sauvanaud, L.; O'Connor, P. *J. Catal.* **2007**, *247*, 307–327.

(15) Domine, M. E.; Iojoiu, E. E.; Davidian, T.; Guilhaume, N.; Mirodatos, C. *Catal. Today* **2008**, *133–135*, 565–573.

(16) Lappas, A. A.; Bezergianni, S.; Vasalos, I. A. *Catal. Today* **2009**, *145*, 55–62.

(17) Bertero, M.; Sedran, U. *Bioresour. Technol.* **2013**, *135*, 644–651.

(18) Rioche, C.; Kulkarni, S.; Meunier, F. C.; Breen, J. P.; Burch, R. *Appl. Catal., B* **2005**, *61*, 130–139.

(19) Basagianis, A. C.; Verykios, X. E. *Appl. Catal., A* **2006**, *308*, 182–193.

(20) Bimbela, F.; Oliva, M.; Ruiz, J.; García, L.; Arauzo, J. *J. Anal. Appl. Pyrolysis* **2007**, *79*, 112–120.

(21) Bimbela, F.; Oliva, M.; Ruiz, J.; García, L.; Arauzo, J. *J. Anal. Appl. Pyrolysis.* **2009**, *85*, 204–213.

(22) Bimbela, F.; Chen, D.; Ruiz, J.; García, L.; Arauzo, J. *Appl. Catal., B* **2012**, *119–120*, 1–12.

(23) Ramos, M. C.; Navascués, A. I.; García, L.; Bilbao, R. *Ind. Eng. Chem. Res.* **2007**, *46*, 2399–2406.

(24) Medrano, J. A.; Oliva, M.; Ruiz, J.; García, L.; Arauzo, J. *Int. J. Hydrogen Energy* **2009**, *85*, 214–225.

(25) Iwasa, N.; Yamane, T.; Arai, M. *Int. J. Hydrogen Energy* **2011**, *36*, 5904–5911.

(26) Czernik, S.; French, R.; Feik, C.; Chornet, E. *Ind. Eng. Chem. Res.* **2002**, *41*, 4209–4215.

(27) Galdámez, J. R.; García, L.; Bilbao, R. *Energy Fuels* **2005**, *19*, 1133–1142.

(28) Xu, Q.; Lan, P.; Zhang, B.; Ren, Z.; Yan, Y. *Energy Fuels* **2010**, *24*, 6456–6462.

(29) Medrano, J. A.; Oliva, M.; Ruiz, J.; García, L.; Arauzo, J. *Energy* **2011**, *36*, 2215–24.

(30) Li, H.; Xu, Q.; Xue, H.; Yan, Y. *Renewable Energy* **2009**, *34*, 2872–2877.

(31) Zhang, S.; Li, X.; Xu, Q.; Yan, Y. *J. Anal. Appl. Pyrolysis* **2011**, *92*, 158–163.

(32) Yan, C.-F.; Cheng, F.-F.; Hu, R.-R. *Int. J. Hydrogen Energy* **2010**, *35*, 11693–11699.

(33) Oasmaa, A.; Czernik, S. *Energy Fuels* **1999**, *13*, 914–921.

(34) Bertero, M.; de la Puente, G.; Sedran, U. *Energy Fuels* **2011**, *25*, 1267–1275.

(35) Czernik, S.; Evans, R.; French, R. *Catal. Today* **2007**, *129*, 265–268.

(36) Iojoiu, E. E.; Domine, M. E.; Davidian, T.; Guilhaume, N.; Mirodatos, C. *Appl. Catal., A* **2007**, *323*, 147–161.

(37) Wang, Z.; Pan, Y.; Dong, T.; Zhu, X.; Kan, T.; Yuan, L.; Torimoto, Y.; Sadakata, M.; Li, Q. *Appl. Catal., A* **2007**, *320*, 24–34.

(38) Wu, C.; Huang, Q.; Sui, M.; Yan, Y.; Wang, F. *Fuel Process. Technol.* **2008**, *89*, 1306–1316.

(39) van Rossum, G.; Kersten, S. R. A.; van Swaaij, W. P. M. *Ind. Eng. Chem. Res.* **2009**, *48*, 5857–5866.

(40) Kan, T.; Xiong, J.; Li, X.; Ye, T.; Yuan, L.; Torimoto, Y.; Yamamoto, M.; Li, Q. *Int. J. Hydrogen Energy* **2010**, *35*, 518–532.

(41) Gayubo, A. G.; Valle, B.; Aguayo, A. T.; Olazar, M.; Bilbao, J. *J. Chem. Technol. Biotechnol.* **2010**, *85*, 132–144.

(42) Valle, B.; Remiro, A.; Olazar, M.; Bilbao, J.; Gayubo, A. G. *Int. J. Hydrogen Energy* **2013**, *38*, 1307–1318.

(43) Remiro, A.; Valle, B.; Aguayo, A. T.; Bilbao, J.; Gayubo, A. G. *Fuel Process. Technol.* **2013**, *115*, 222–232.

(44) Yan, C. F.; Hu, E. Y.; Cai, C. L. *Int. J. Hydrogen Energy* **2010**, *35*, 2612–2616.

(45) Remiro, A.; Valle, B.; Aramburu, B.; Aguayo, A. T.; Bilbao, J.; Gayubo, A. G. *Ind. Eng. Chem. Res.* **2013**, DOI: 10.1021/ie4021705.
(46) Fernández-Akarregi, A. R.; Makibar, J.; López, G.; Amutio, M.; Olazar, M. *Fuel Process. Technol.* **2013**, *112*, 48−56.
(47) Amutio, M.; Lopez, G.; Aguado, R.; Artetxe, M.; Bilbao, J.; Olazar, M. *Fuel* **2012**, *95*, 305−311.
(48) Amutio, M.; Lopez, G.; Aguado, R.; Bilbao, J.; Olazar, M. *Energy Fuels* **2012**, *26*, 1353−1362.
(49) Alberton, A. L.; Souza, M. M. V. M.; Schmal, M. *Catal. Today* **2007**, *123*, 257−264.
(50) Gayubo, A. G.; Valle, B.; Aguayo, A. T.; Olazar, M.; Bilbao, J. *Ind. Eng. Chem. Res.* **2010**, *49*, 123−131.
(51) Valle, B.; Gayubo, A. G.; Aguayo, A. T.; Olazar, M.; Bilbao, J. *Energy Fuels* **2010**, *24*, 2060−2070.
(52) Ereña, J.; Sierra, I.; Olazar, M.; Gayubo, A. G.; Aguayo, A. T. *Ind. Eng. Chem. Res.* **2008**, *47*, 2238−2247.
(53) Sierra, I.; Ereña, J.; Aguayo, A. T.; Arandes, J. M.; Olazar, M.; Bilbao, J. *Appl. Catal., B* **2011**, *106*, 167−173.
(54) Valle, B.; Castaño, P.; Olazar, M.; Bilbao, J.; Gayubo, A. G. *J. Catal.* **2012**, *285*, 304−314.
(55) Bartholomew, C. H. *Appl. Catal., A* **2001**, *212*, 17−60.
(56) Wang, D.; Czernik, S.; Montané, D.; Mann, M.; Chornet, E. *Ind. Eng. Chem. Res.* **1997**, *36*, 1507−1518.
(57) Davidian, T.; Guilhaume, N.; Iojoiu, E.; Provendier, H.; Mirodatos, C. *Appl. Catal., B* **2007**, *73*, 116−127.
(58) van Rossum, G.; Kersten, S. R. A.; van Swaaij, W. P. M. *Ind. Eng. Chem. Res.* **2007**, *46*, 3959−3967.
(59) Hou, T.; Yuan, L.; Ye, T.; Gong, L.; Tu, J.; Yamamoto, M.; Tirimoto, Y.; Li, Q. *Int. J. Hydrogen Energy* **2009**, *34*, 9095−9107.
(60) Seyedeyn-Azad, F.; Salehi, E.; Abedi, J.; Harding, T. *Fuel Process. Technol.* **2011**, *92*, 563−569.
(61) Salehi, E.; Seyedeyn-Azad, F.; Harding, T.; Abedi, J. *Fuel Process. Technol.* **2011**, *92*, 2203−2210.
(62) Zhang, Y.; Li, W.; Li, Q.; Xu, Q.; Yan, Y. *Chem. Eng. Technol.* **2012**, *35*, 302−308.
(63) Seyedeyn-Azad, F.; Abedi, J.; Harding, T. *Chem. Eng. J.* **2012**, *180*, 145−150.